Modeling of heat and high viscous fluid distributions with variable viscosity in a permeable channel

Jacques Hona*

Applied Mechanics Laboratory, Faculty of Science, University of Yaoundé I, P.O. Box 7389, Yaoundé, Cameroon

ABSTRACT

The flow field under study is characterized by velocity components, temperature and pressure in non-dimensional formulation. The flow is driven by suction through the horizontal channel with permeable walls fixed at different temperatures. In order to ascertain a better understanding of the dynamic behavior of the flow, the Navier-Stokes equations and the energy equation are solved concurrently applying a similarity transformation technique. The hydrodynamic structures obtained from the numerical integration include flow reversal or backward flow, collision zones due to the coexistence of wall suction and flow reversal inside the channel, the inflection through temperature distribution, the growth of thermal gradients near the walls, and the sensitivity of normal pressure gradients to the difference of temperatures at boundaries. These hydrodynamic structures are investigated considering the influences of the Péclet number P and the sensitivity of viscosity to thermal variations α which are the main control parameters of the problem.

Keywords: Two-dimensional channel flows, Creeping flows, Variable viscosity, Similarity method, Nonlinear two-point boundary-value problem, Numerical solutions

1. INTRODUCTION

The theoretical investigations of flows which develop within porous channels or tubes are achieved by many scientists using the Navier-Stokes equations. These equations derive from the conservations of mass and momentum. The Navier-Stokes equations also known as the momentum equation are described by the velocity field components. The flow may be three-dimensional or two-dimensional. In the first case, the flow is characterized by all the three components of the velocity field. This case is usually encountered and highlights the reality of some natural fluid motions but not reveals many rich hydrodynamic structures through the recent literature about laminar flow processes [1, 2]. The second case is increasingly considered since direct industrial applications are related to two-dimensional flows which have also gained many theoretical and experimental supports in order to ascertain their deeper understanding. These applications include petroleum industry, paper manufacturing, filtration, irrigation, solar energy collectors, the boundary layer separation with suction or injection, the separation of a binary mixture by gaseous diffusion, and purification in the

^{*}Corresponding Author: E-mail: honajacques@yahoo.fr

biopharmaceutical industry. Indeed, the flow is assumed to be two-dimensional when the velocity field presents the same behavior along a given direction, and is thereby described by two components.

The pioneer work about a two-dimensional porous channel flow is the study of Berman [3] which provides a valuable method of solution called the similarity technique that many scientists [4–9] are making increasing use for investigating flows between two permeable walls. When the channel is porous or admits wall motion, or both, the flow is denoted as Berman flow by some authors.

The similarity technique is an indirect approach of seeking solution; such that, instead of finding the velocity field itself which describes the Navier-Stokes equations for a given two-dimensional flow, a single function related to the velocity components is adopted and its corresponding differential equation is derived. The noted function which satisfies mass conservation is defined in order to verify the boundary conditions of the problem and by taking into consideration the geometry of the channel. After yielding the evolution of this function, the velocity components can be derived.

The similarity transformation of the Navier-Stokes equations introduced by Berman [3] is later on widely used for studying flows through porous rectangular channels [10–15] and cylindrical conducts [16–20]. In addition, when thermal effects are considered in the flow domain, the energy equation is associated with the Navier-Stokes equations to model the problem and a Berman type similarity solution can also be derived [21–27].

The present study is devoted to examine a creeping flow through a channel with two porous walls kept at different temperatures. In fact, the creeping flow occurs when the fluid is assumed highly viscous, so that inertial terms of the momentum equation are neglected compared to viscous ones [28–29]. The temperature difference between the walls of the channel causes the exponential variation of the dynamic viscosity. This variation couples the Navier-Stokes equations to the energy equation. The desire is to investigate some hydrodynamic structures due to variable high viscosity not considered in previous works. The similarity technique is used to transform the Navier-Stokes equations and the energy equation into two nonlinear ordinary differential equations which are then solved applying the shooting technique associated with the fourth-order Runge-Kutta algorithm. The validity of the numerical scheme is tested using the comparison of numerical results obtained for low values of control parameters with the zero-order analytical solution. For adding clarity, the efficiency of the numerical code is accepted if the numerical results approach the analytical solution. The hydrodynamic structures obtained from the flow field characteristics enable to extend the solution range to relevant physical meaning.

The paper is organized as follows: Section 2 is about the model equations and a similarity transformation approach. Sections 3 and 4 deal with the analytical approach for low values of control numbers and the validity of the numerical scheme, respectively; while Section 5 is reserved to the results analysis. Section 6 is devoted to the conclusion.

2. PROBLEM FORMULATION

The creeping flow occurs between two horizontal rigid planes. Both planes which are the walls of the channel are parallel and uniformly permeable. In addition, the two planes are distanced by 2 h known as the width of the channel which is small compared to the height. The suction speed at walls V is assumed to be positive. The temperature at the cold wall is T_0 and that of the hot wall is T_1 , such that $T_1 > T_0$. The physical properties of the fluid are the specific mass ρ , the thermal conductivity κ , and the temperature-dependent viscosity μ which takes the value μ_0 at temperature T_0 . The non-dimensional variables in terms of length,

velocity, temperature, pressure, and viscosity are measured in units of (h), (V), $(\Delta T = T_1 - T_0)$, (ρV^2) , and (μ_0) , respectively. Thus, the Reynolds number $R = \rho V h / \mu_0$ and the Péclet number $P = \rho V h / \kappa$ are derived. In all that follows, the variables are dimensionless.

A plane Cartesian coordinate system (x, y) is considered, with the origin placed in the center of the channel, such that x represents the coordinate in the streamwise direction, and y is the transverse coordinate as shown in Fig. 1. The x-axis is parallel to the walls and the length of the channel along this axis tends to infinity in order to neglect the influence at the ends. The channel is horizontal, such that gravity has no considerable effects on the fluid flow. The flow is assumed to be two-dimensional, so the velocity field has components as (u, v), where u is the streamwise velocity and v denotes the transverse or the normal velocity. On the other hand, t and t0 are the variables describing temperature and pressure, respectively.

The fluid is supposed highly viscous, such that inertial terms can be ignored. Considering the plane Cartesian geometry and the above non-dimensional variables the problem is described by differential terms as follows:

$$\frac{\partial u}{\partial x} + \frac{\partial v}{\partial y} = 0 \tag{1}$$

$$\frac{\partial p}{\partial x} = \frac{2}{R} \frac{\partial}{\partial x} \left(\mu \frac{\partial u}{\partial x} \right) + \frac{1}{R} \frac{\partial}{\partial y} \left(\mu \frac{\partial u}{\partial y} + \mu \frac{\partial v}{\partial x} \right)$$
 (2)

$$\frac{\partial p}{\partial y} = \frac{1}{R} \frac{\partial}{\partial x} \left(\mu \frac{\partial u}{\partial y} + \mu \frac{\partial v}{\partial x} \right) + \frac{2}{R} \frac{\partial}{\partial y} \left(\mu \frac{\partial v}{\partial y} \right)$$
(3)

$$u\frac{\partial T}{\partial x} + v\frac{\partial T}{\partial y} = \frac{1}{P} \left(\frac{\partial^2 T}{\partial x^2} + \frac{\partial^2 T}{\partial y^2} \right) \tag{4}$$

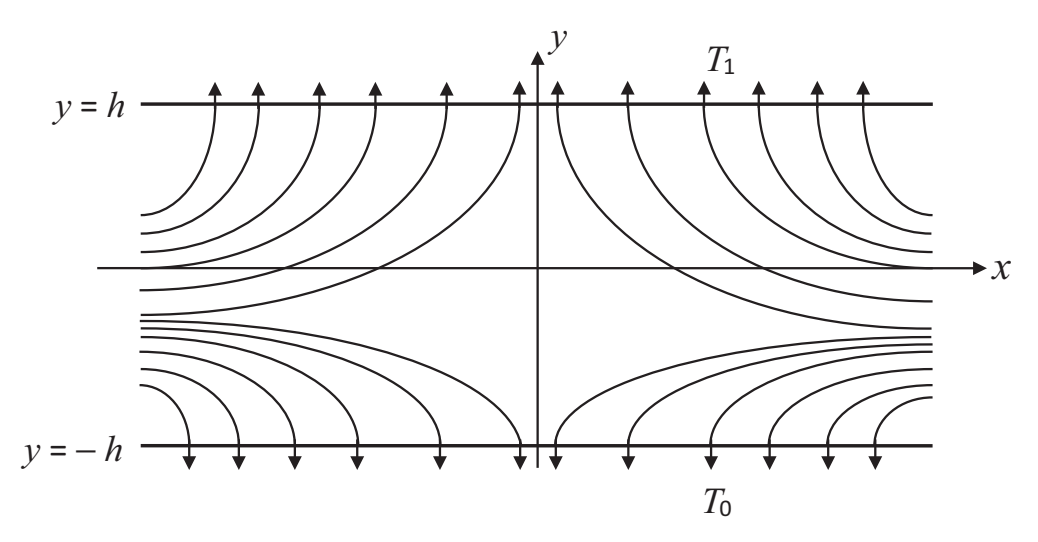


Figure 1: Typical plot of the horizontal channel showing some streamlines and suction occurring at walls

where eqn (1) is the continuity equation, eqns (2) and (3) represent the Navier-Stokes equations, and eqn (4) describes the energy equation. The boundary conditions express the no-slip condition, the equal fluxes and the difference of temperatures at walls:

$$u = 0, v = -1 \text{ and } T = \frac{T_0}{T_1 - T_0}, \text{ for } y = -1$$

$$u = 0, v = +1 \text{ and } T = \frac{T_1}{T_1 - T_0}, \text{ for } y = 1$$
(5)

Due to the two-dimensional configuration of the problem, the introduction of the stream function F in the governing equations is usual. The existence of the stream function F by similarity transformation is associated with new functions θ , A and Q uniform to temperature and pressure gradients, respectively. In addition, a detailed relationship of viscosity with temperature is needed to complete the statement of the problem. For this, the literature offers several possible choices; the usual ones are linear [24, 31], algebraic [23, 31] or exponential behaviors [24–26]. The exponential law is suitable to the problem under study, and the new functions are expressed as:

$$u = x \frac{\partial F}{\partial y}, \qquad v = -F(y)$$

$$T(x, y) = \theta(y) - \left(1 - T_1/T_0\right)^{-1}$$

$$A = \frac{1}{x} \frac{\partial p}{\partial x}, \qquad Q(y) = \frac{\partial p}{\partial y}$$

$$\mu(\theta) = \exp(-\alpha \theta)$$
(6)

where the non-dimensional parameter $\alpha = -(\partial \mu / \partial \theta)/\mu$ is a measure of the sensitivity of viscosity to thermal variations; it depends on the fluid properties and on the temperature difference between the walls. It follows that, the dimensional viscosity varies between the values μ_0 at the cold wall (y = -1), and $\mu_0 \exp(-\alpha)$ at the hot one (y = 1). Positive values of the parameter α correspond to fluids whose viscosity decreases with temperature, the case of most liquids. Negative values of α are in accordance with fluids where viscosity increases with temperature, the case of some gases. Uniform viscosity corresponds to the case where $\alpha = 0$.

The relationships of the non-dimensional velocity components u and v with the stream function F agree with the continuity equation, and the new temperature field θ is suitable to the boundary conditions. According to the geometrical configuration of the channel, the above definitions about the axial pressure gradient per unit length A and the normal pressure gradient Q are in accordance with the momentum conservation.

The curl of the momentum equation produces the vorticity transport process satisfied by F, while function θ describes the similarity energy conservation. This set of differential equations is given as follows:

$$F^{(4)} - 2\alpha\theta^{(1)}F^{(3)} + \alpha(PF + \alpha\theta^{(1)})\theta^{(1)}F^{(2)} = 0$$

$$\theta^{(2)} + PF\theta^{(1)} = 0$$
(7)

with the following boundary conditions:

$$F(-1) = 1,$$
 $F^{(1)}(-1) = 0,$ $\theta(-1) = 0$ (8)
 $F(1) = -1,$ $F^{(1)}(1) = 0,$ $\theta(1) = 1$

where $F^{(i)} = d^i F/dy^i$, and $\theta^{(i)} = d^i \theta/dy^i$.

The expressions about pressure gradients are derived as:

$$Q(y) = (2\alpha\theta^{(1)}F^{(1)} - F^{(2)})\exp(-\alpha\theta)/R$$
(9)

$$A = \left(F^{(3)} - \alpha \theta^{(1)} F^{(2)}\right) \exp(-\alpha \theta) / R = \text{constant}$$
 (10)

The problem stated in eqns (7) and (8) is a nonlinear two-point boundary-value problem. The nonlinearity of the differential equations of the problem is due to the correlations in terms of the stream function and thermal gradients. These correlations are due themselves to the dependence of the dynamic viscosity on temperature.

3. FLOW CHARACTERISTICS FOR SMALL VALUES OF CONTROL NUMBERS

Low Péclet numbers provide an analytical solution of the problem which helps while testing the validity of the numerical scheme in Section 4. In this investigation, the strategy consists to find the analytical solution of the flow by writing the non-dimensional stream function F, and the non-dimensional temperature θ , as Taylor series expansions in terms of small P. One gets:

$$F(y) = F_0(y) + PF_1(y) + ...$$

$$\theta(y) = \theta_0(y) + P\theta_1(y) + ...$$
(11)

The couple (F_0, θ_0) is the zero-order analytical solution of the flow which satisfies the boundary conditions. That is:

$$F_0(y) = C_1 + C_2 y + (C_3 + C_4 y) \exp\left(\frac{\alpha}{2}y\right)$$

$$\theta_0(y) = (y+1)/2$$
(12)

where C_1 , C_2 , C_3 and C_4 are the constants of integration given by:

$$C_1 = (2\alpha + 2\sinh(\alpha))/\Delta, \quad C_2 = \alpha^2/\Delta$$

$$C_3 = -(2\alpha\cosh(\alpha/2) + 4\sinh(\alpha/2))/\Delta, \quad C_4 = 2\alpha\sinh(\alpha/2)/\Delta$$

with $\Delta = 4 \sinh^2(\alpha/2) - \alpha^2$. It appears that, as the Péclet number tends to zero, the non-dimensional temperature undergoes a linear law inside the channel. Since the zero-order analytical solution (F_0, θ_0) satisfies the boundary conditions of the problem; then the first-order analytical solution (F_1, θ_1) verifies the zero boundary conditions, and does not

influence the dynamics discussed in this work. After finding solutions for F_0 and θ_0 , expressions from eqns (9) and (10) enable to derive the corresponding transverse pressure gradient and axial pressure gradient per unit length. One obtains:

$$Q_0 = \frac{1}{R} \left(\frac{\alpha^2}{4} (C_3 + C_4 y) + \alpha C_2 \exp\left(-\frac{\alpha}{2} y\right) \right) \exp(-\alpha/2)$$
 (13)

$$A_0 = \frac{\alpha^2}{4R} C_4 \exp(-\alpha/2) = \text{constant}$$
 (14)

In Fig. 2 is plotted function F_0 from the formulas (12), for different values of the parameter α , and the zero-order normal pressure gradient Q_0 is presented in Fig. 3 using the formula (13), for R=1. In addition, if the viscosity is uniform ($\alpha=0$) in the case where P=0, the investigation is reduced to a linear problem which provides an analytical solution as follows: $F=(y^3-3y)/2$ and $\theta=(y+1)/2$.

4. VALIDITY OF THE NUMERICAL SCHEME

The numerical integration is based on the shooting method associated with the fourth-order Runge-Kutta algorithm [22]. The nonlinear two-point boundary-value problem (7) and (8) is transformed into an initial-value one. Since three of the six auxiliary conditions are of the boundary value type, a numerical solution becomes dependent upon three initial guesses. The fourth-order Runge-Kutta algorithm is applied to solve the obtained initial-value problem as a set of six first-order coupled differential equations with three unspecified start-up conditions among the six initial conditions. In seeking the three unknown initial guesses, an

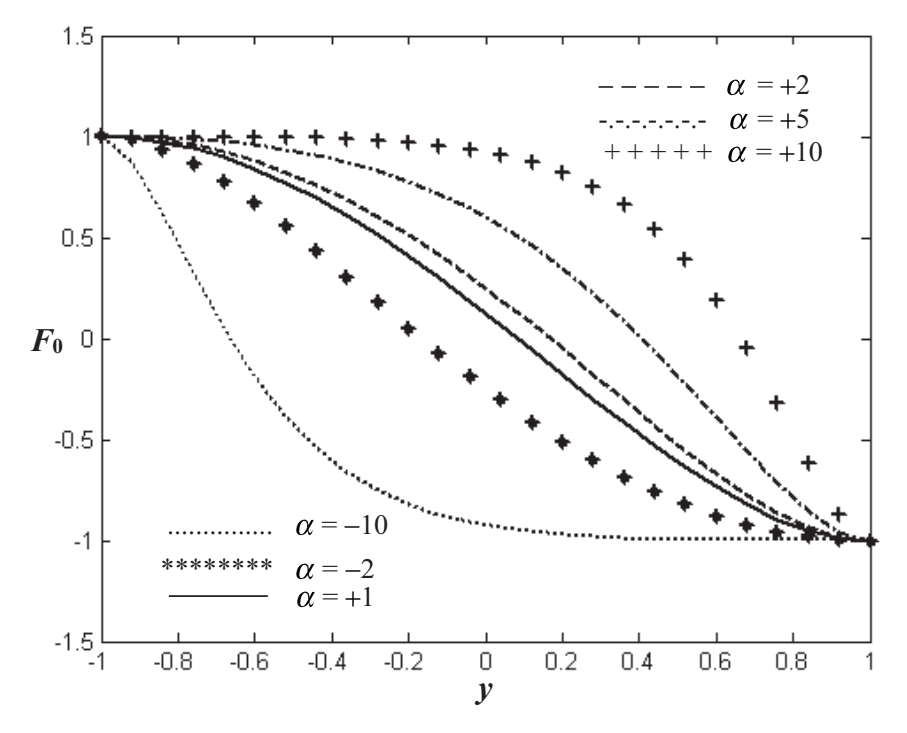


Figure 2: Zero-order analytical solution for the stream function

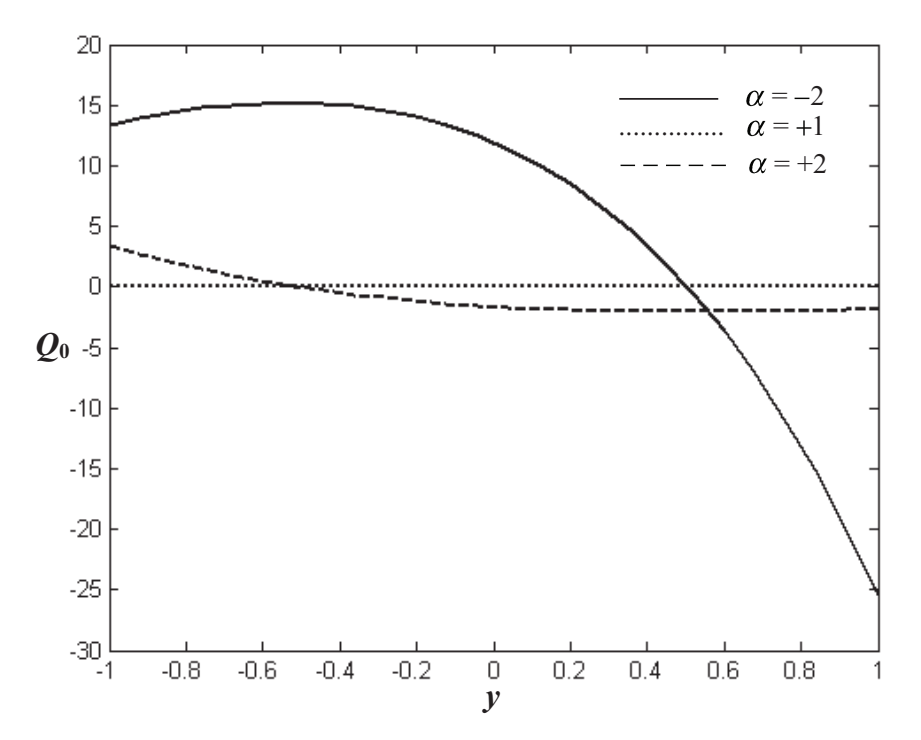


Figure 3: Zero-order analytical solution of the transverse pressure gradient for R=1

optimization type problem is derived and the rapidly converging inverse Jacobian method is applied in an iterative fashion and then, the numerical solution of the problem can be provided.

To test the validity of the numerical scheme, functions θ and F are plotted for small values of the Péclet number by setting $\alpha=-2$. In that case, the numerical solution obtained must agree with the analytical solution found in Section 3. It appears that for small values of the Péclet number, the numerical solution tends to the zero-order analytical solution as shown in Fig. 4, where the dash-dot curve is nearly identical to the solid line which corresponds to the analytical solution for the non-dimensional temperature. On the other hand, different scales are adopted in Fig. 5 in order to make the asymptotic curves distinguishable as the solution branches for the non-dimensional stream function tend to a same constant curve.

The problem is fully influenced by the Péclet number and the sensitivity of viscosity to thermal variations, instead of the Reynolds number as usual. This behavior is in accordance with the creeping flows where the contribution of the Reynolds number is reduced. For this reason, the Péclet numbers are low and moderate because the flow occurs with weak velocities.

5. NUMERICAL RESULTS ANALYSIS

First of all, it is relevant to note that, the problem admits a basic solution in terms of velocity components on the form:

$$u(x, y) = x \frac{\partial F}{\partial y}$$

$$v(x, y) = -F(y)$$
(15)

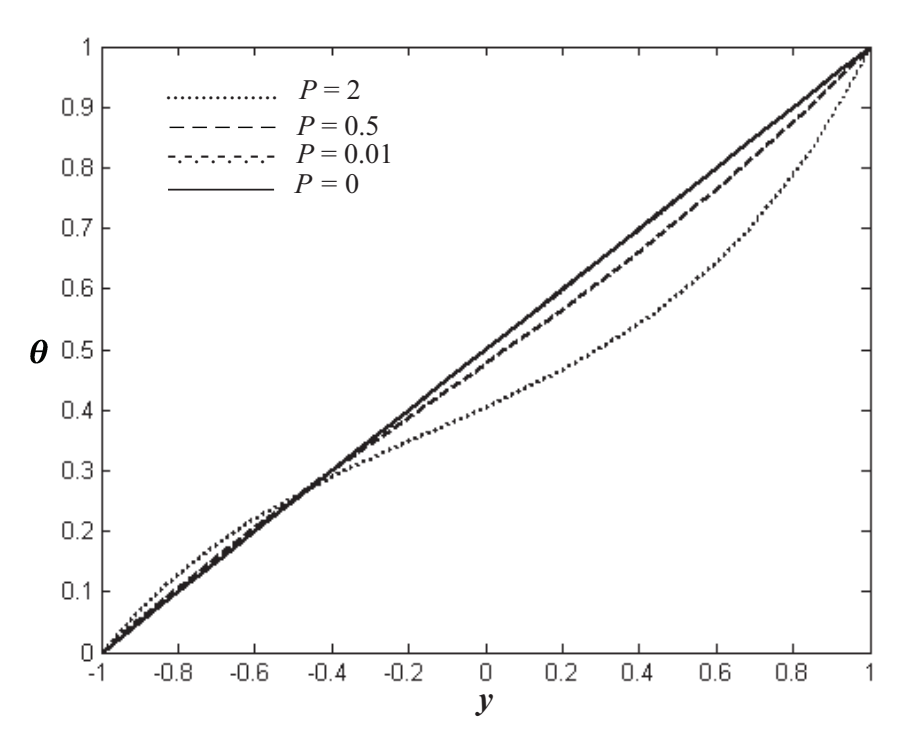


Figure 4: Comparison of the numerical solution with the zero-order analytical solution for the non-dimensional temperature field by setting $\alpha = -2$

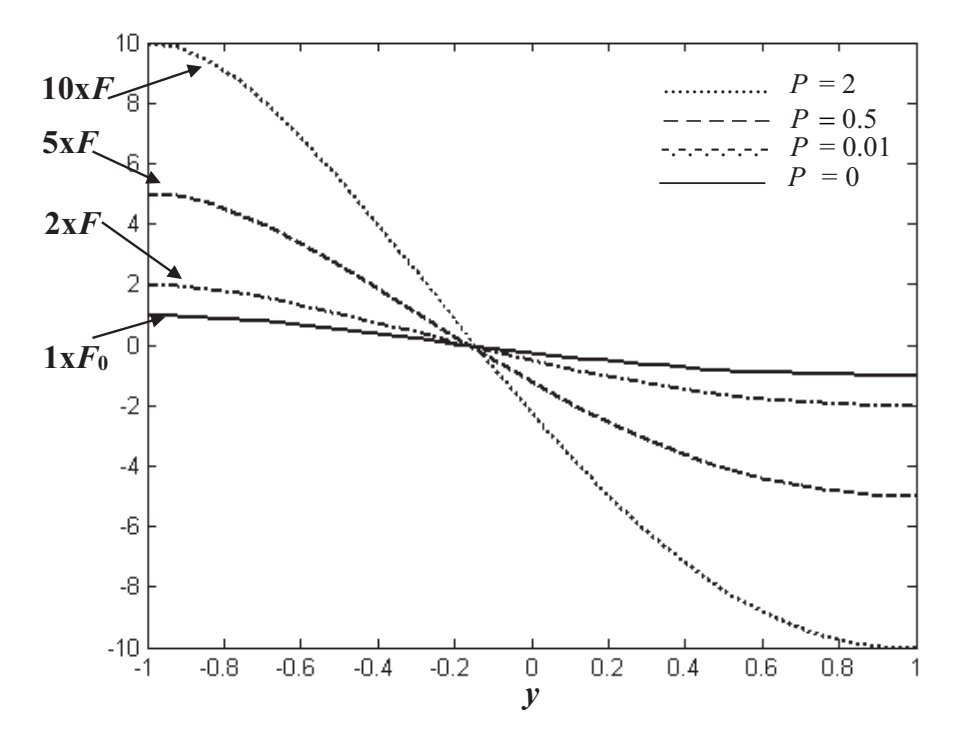


Figure 5: Comparison of the numerical solution with the zero-order analytical solution for the non-dimensional stream function by setting $\alpha = -2$

This solution which satisfies the boundary conditions agrees with the Taylor profile modified by the dependence of viscosity on temperature, but is not the complete solution of differential equations of the current investigation. In three-dimensional computation procedure, Fig. 6 shows that the streamwise velocity is influenced by the two space variables and presents a parabolic behavior with the increase of x. On the other hand, the basic normal velocity distribution as presented in Fig. 7 does not vary enough along the streamwise direction; this behavior agrees with the pioneer assumption of Berman. For adding clarity, the 2D-plots are convenient for further results which follow in this study since the streamwise coordinate does not describe the similarity functions F and θ of the problem.

After finding solutions for the non-dimensional stream function and the non-dimensional temperature, the solutions about velocity components are derived applying the similarity property of eqns (6). At this stage, the importance to use the similarity method is confirmed, because it enables the transformation of the four differential eqns (1)–(4) relative to velocity components and temperature into a set of two coupled eqns (7) satisfied by the stream function and a similarity function for the temperature field.

Inside the channel, Fig. 8(a) shows that, for a given conductivity, the normal velocity decreases with the sensitivity of viscosity to thermal variations. Hence, the increase of the parameter α is not favorable to suction. The distribution of the normal velocity under different conductivities depends on the sign of the fixed parameter α . Indeed, Fig. 8(b) reveals that, moderate Péclet numbers are adverse to suction in the case of a negative fixed sensitivity of viscosity to thermal variations. But a contrary behavior is observed in Fig. 8(c) with a positive fixed sensitivity of viscosity to thermal variations. On the other hand, the mass withdrawal phenomenon which occurs at walls due to suction is accompanied with flow reversal process also known as backward flow within the channel. For clarity, the

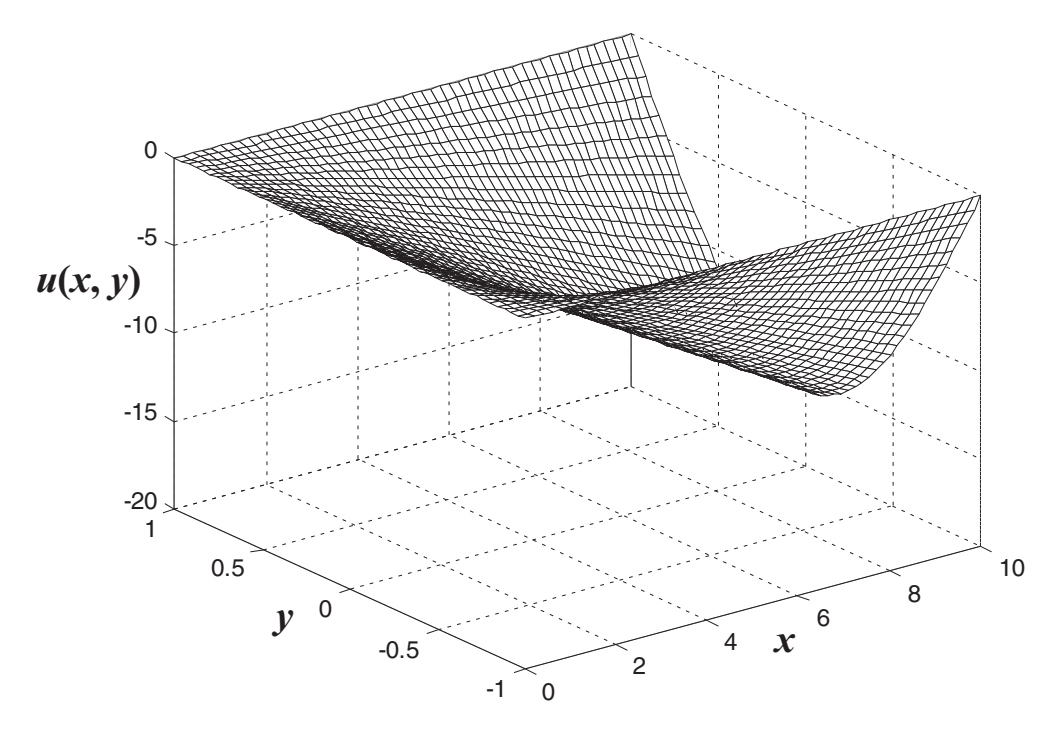


Figure 6: Basic streamwise velocity showing a parabolic behavior as the streamwise coordinate increases

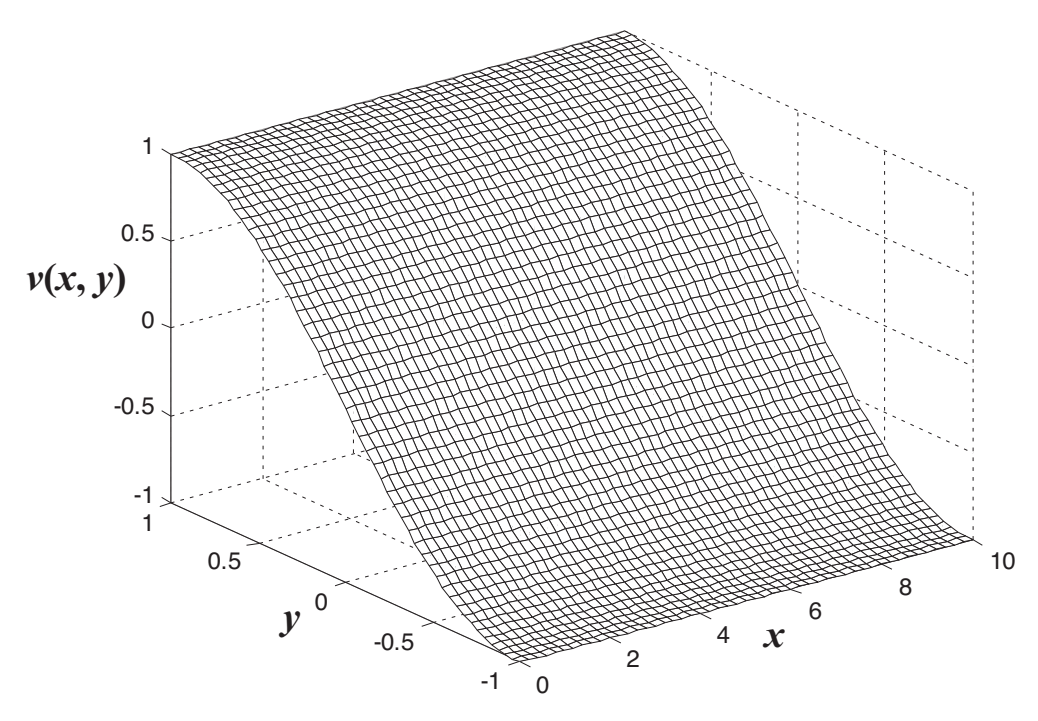


Figure 7: Basic normal velocity satisfying the Taylor profile

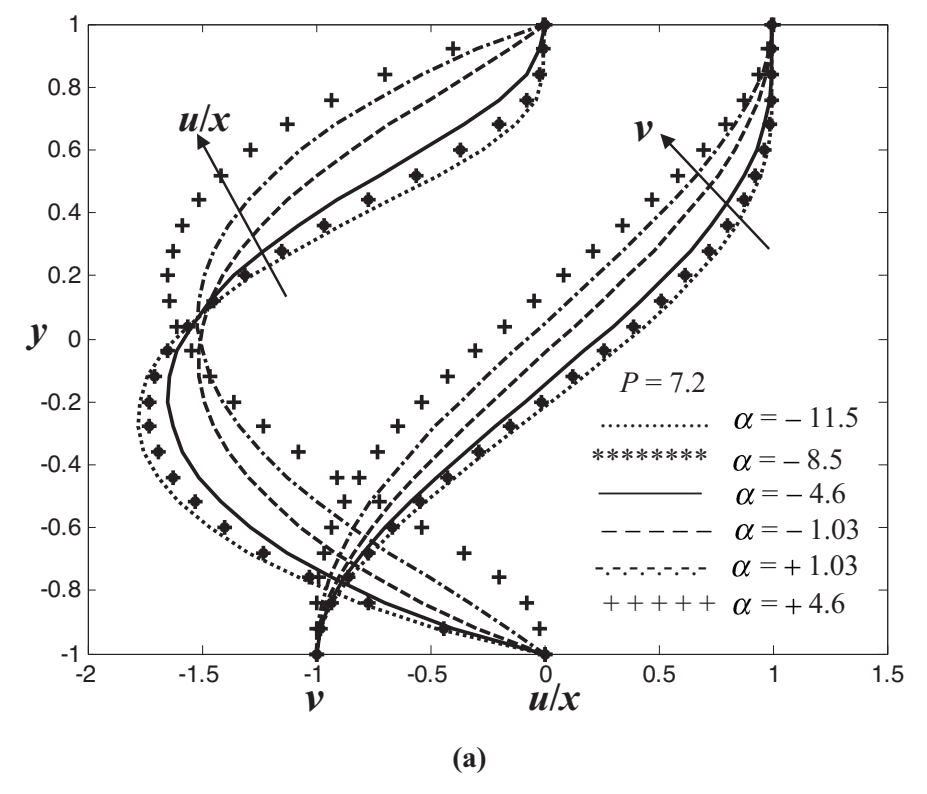


Figure 8: (Continued)

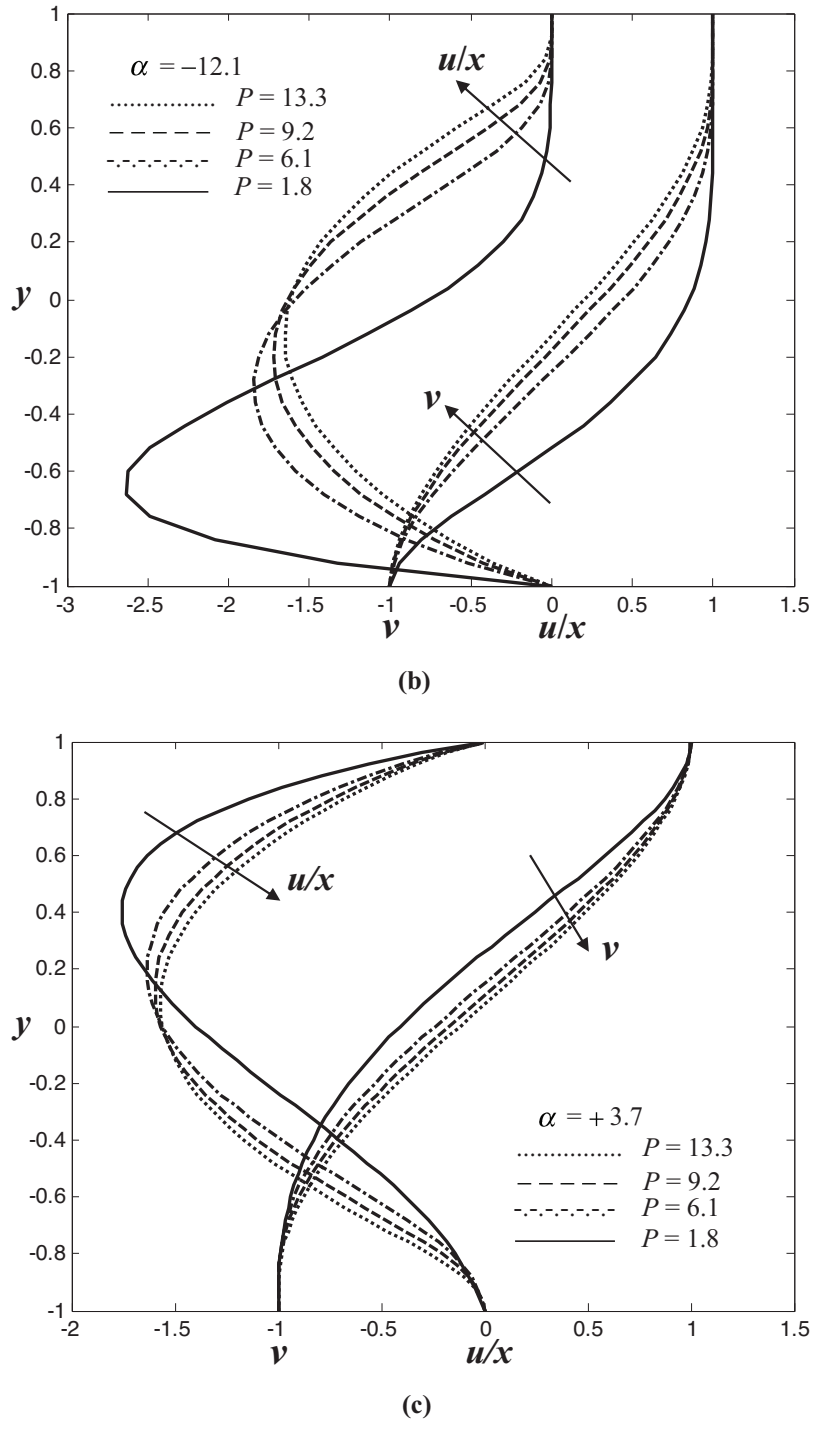


Figure 8: Normal velocity and streamwise velocity per unit length: (a) for P=7.2 under various values of the sensitivity of viscosity to thermal variations, (b) for $\alpha=-12.1$ under different values of the Péclet number, (c) for $\alpha=+3.7$ under different conductivities

scenario of the reverse flow manifests itself by negative streamwise velocities per unit length as shown in Fig. 8. However, the existence of the normal velocity for different values of parameters confirms the opposing behaviors between suction and flow reversal. These opposing effects in the channel are due to the high viscosity of the fluid which gives rise to important viscous stresses, such that the motion of fluid particles is slowed enough in light of Fig. 8.

There are some zones of intersection through the axial velocity distribution where the effects caused by different values of control numbers are identical as shown in Fig. 8. That is because the high viscosity of the fluid is able to create some regions having the same dynamic behavior within the channel. The streamwise velocity per unit length presents a parabolic behavior which involves the dominance of the backward flow on suction. In addition, the solution branches corresponding to P = 1.8 in Fig. 8(b), show a minimum value of the axial velocity per unit length and the maximum normal velocity. These behaviors are due to the simultaneous presence of suction and flow reversal with an attempt to create some collision zones in the channel as found in previous studies [18, 30].

The distribution of thermal gradients in the channel through Fig. 9 reveals the location of the maxima at walls. That is because suction increases the thermal gradients at walls. Furthermore, the minima of these thermal gradients are situated around the middle of the flow region, because the temperature does not vary enough at the vicinity of the center of the channel. In Fig. 9(a), a solution branch with the maximum value at the cold wall is the one with the minimum value near the hot wall. Every curve of Fig. 9(b) presents its respective maximum at the hot wall for a fixed negative sensitivity of viscosity to thermal variations.

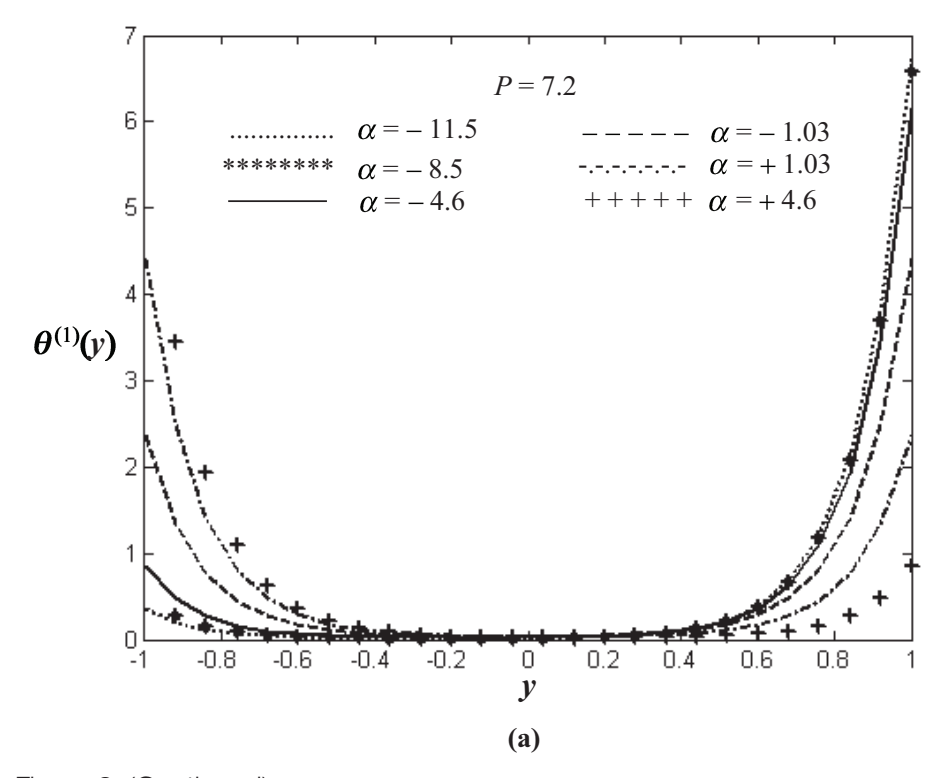
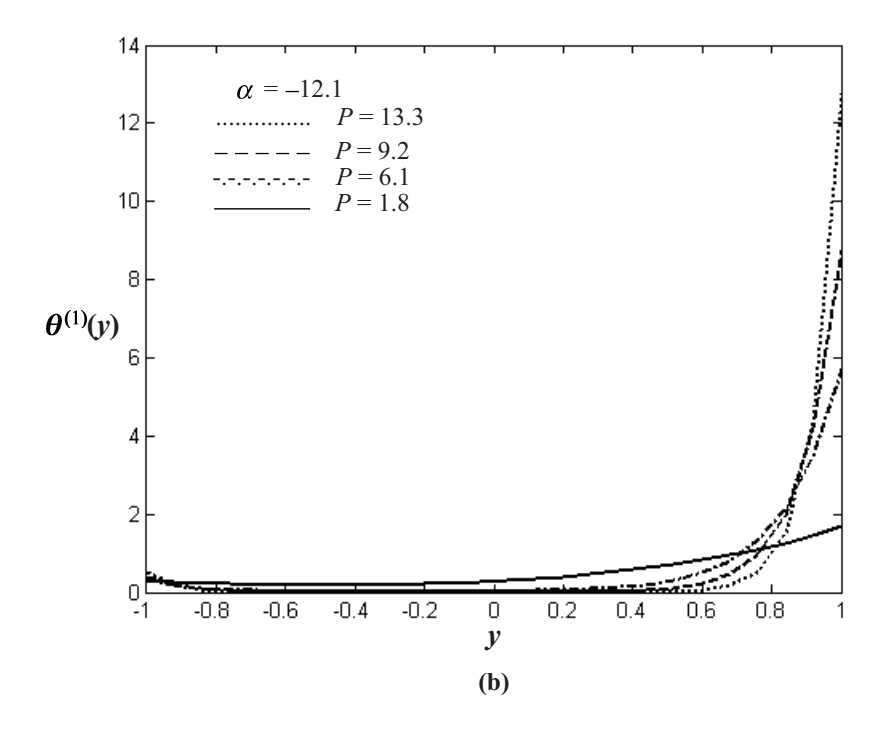


Figure 9: (Continued)



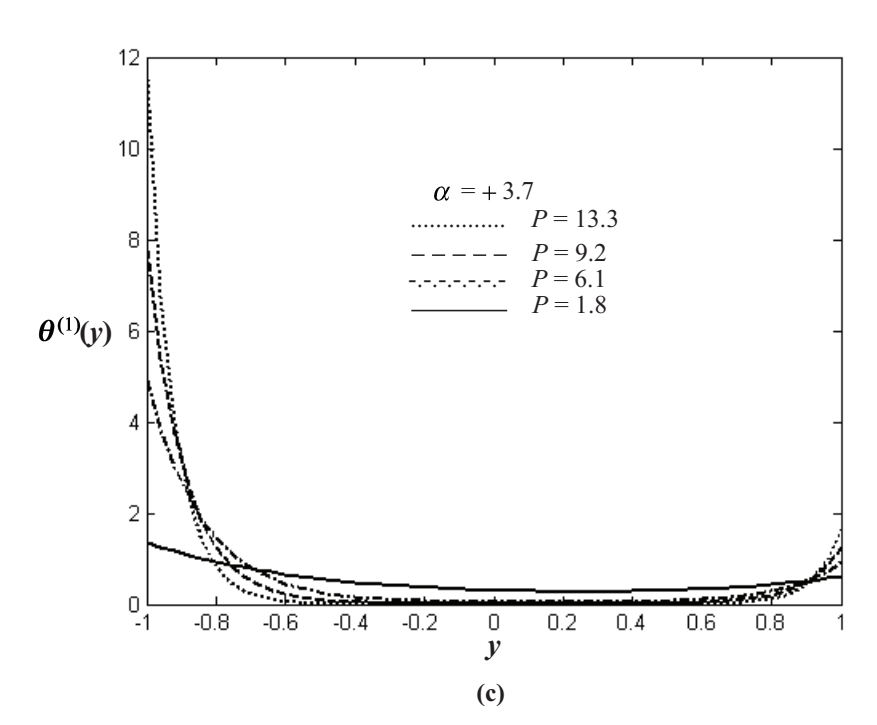


Figure 9: Thermal gradients distribution: (a) for P=7.2 under various values of the sensitivity of viscosity to thermal variations, (b) for $\alpha=-12.1$ under different values of the Péclet number, (c) for $\alpha=+3.7$ under different conductivities

However, the maxima of these curves move from the hot wall to the cold one when the parameter α takes a positive value as illustrated in Fig. 9(c). The noted permutation highlights the exchange of behavior with respect to the maxima of thermal gradients between the two walls. This exchange of behavior is due to the sign of the parameter α and the difference of temperatures at boundaries. In all cases, for each curve, function $\theta^{(1)}(y)$ decreases near the cold wall, and increases in the neighborhood of the hot wall as function of the normal coordinate y.

Important variations of temperature in Fig. 10(a) are observed near the walls due to suction, but the curves are almost horizontal away from the walls. For this fact, the growth of temperature reveals two concavities. The first concavity, situated at the vicinity of the cold wall, is turned toward the stocking; and the second concavity, located in the neighborhood of the hot wall is turned toward the top, as shown in Fig. 10(a) where is plotted function $\theta(y)$ for different sensitivities of viscosity to thermal variations at fixed conductivity. It follows that, the temperature distribution presents a large area of inflection. Since the temperature is almost constant in a large area around the center of the channel, thermal gradients in that zone tend to zero. In addition, by referring to Fig. 10(a), for a given Péclet number, the temperature increases with the parameter α while the inflection disappears with the decrease of this parameter.

For a fixed negative sensitivity of viscosity to thermal variations, Fig. 10(b) shows the disappearance of the inflection and rapid growths of temperature are only observed near the hot wall. In Fig. 10(b), the temperature increases with the decrease of the Péclet number. The inflection appears again in the case of a fixed positive parameter α as shown in Fig. 10(c) where

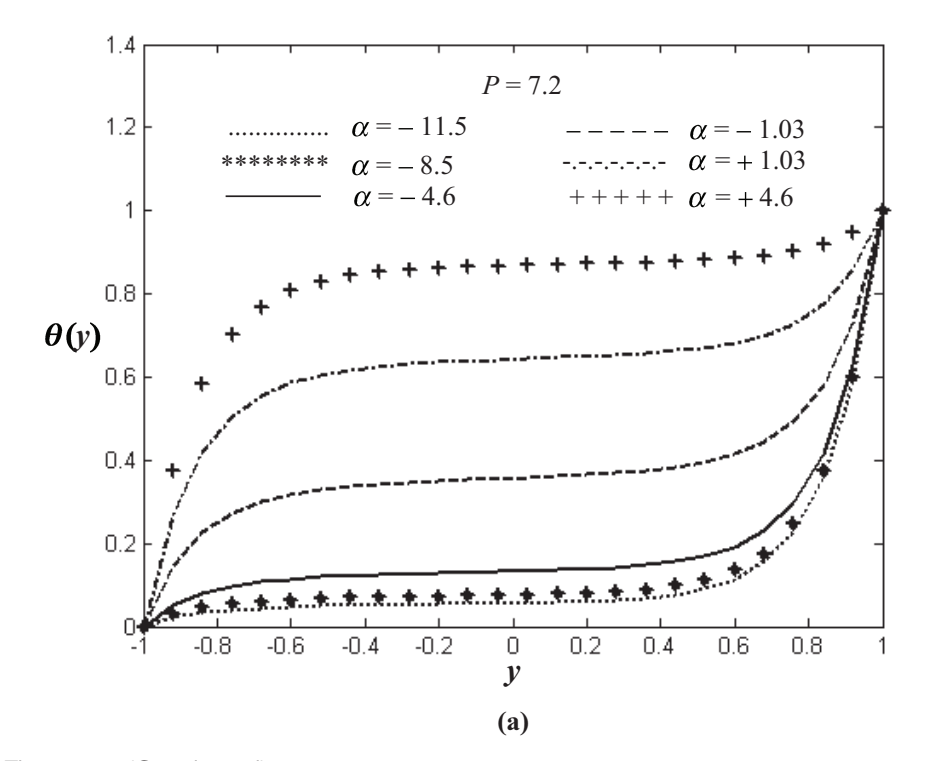


Figure 10: (Continued)

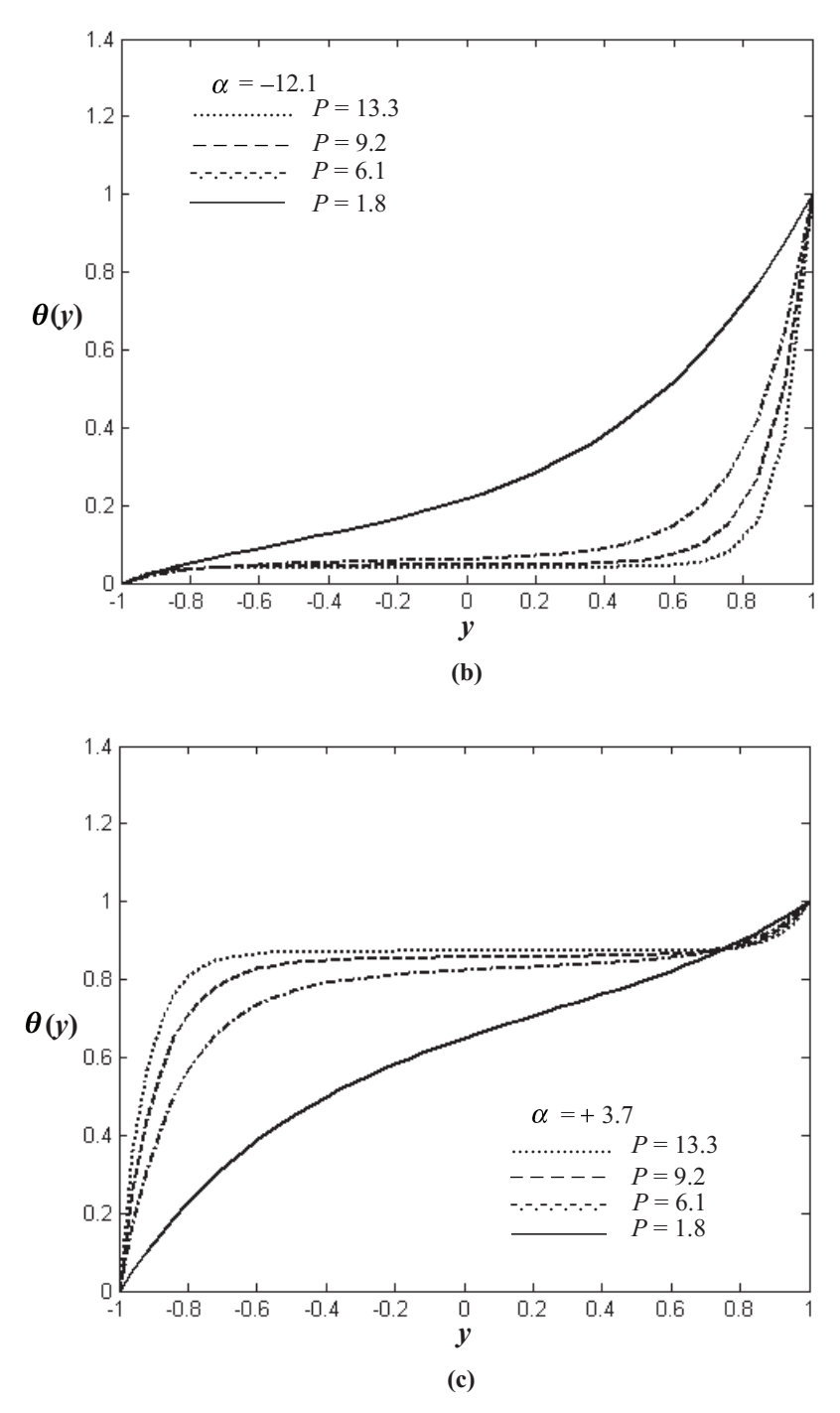


Figure 10: Temperature distribution: (a) for P=7.2 showing a rapid variation at the vicinity of both walls and a large inflection area, (b) for $\alpha=-12.1$ showing rapid variations at the vicinity of the hot wall, (c) for $\alpha=+3.7$ showing rapid variations at the vicinity of the cold wall and a large inflection area

function $\theta(y)$ is plotted for different conductivities and presents rapid variations only at the vicinity of the cold wall. Figures 10(b) and 10(c) show that the temperature distribution in the channel tends to the linear law with the decrease of the Péclet number as found in Section 3.

For clarity, the rapid growth of temperature observed near the walls in Fig. 10(a), and only near the cold wall in Fig. 10(c), disappears in the neighborhood of the cold wall in Fig. 10(b), because the low temperature is not sensitive to the changes happening with respect to the conductivity in the case of a fixed high negative sensitivity of viscosity to thermal variations.

The data about pressure gradients can be obtained by setting R = 1 from the formulas (9) and (10) after solving the vorticity equation and the energy equation. It is important to signal that, in this study, the pressure in the flow region exists only in terms of pressure difference, pressure gradients are then derived and inform about pressure variation rates inside the channel. Furthermore, a fixed reference value is required in order to carry out the pressure difference itself. But this fixed reference value does not interest the dynamics discussed in this work.

In light of Fig. 11(a), the maxima of the normal pressure gradients are located away from the walls; this is most noticeable for $\alpha = -11.5$, $\alpha = -8.5$ and $\alpha = -4.6$ because normal pressure gradients increase near the cold wall and decrease near the hot wall at fixed conductivity. In addition, through the channel, in the case of fixed conductivity, normal pressure gradients diminish with the sensitivity of viscosity to thermal variations. In Fig. 11(b), function Q which is plotted under different conductivities at a fixed negative parameter α , shows that the normal pressure gradient is very sensitive to high temperature for high

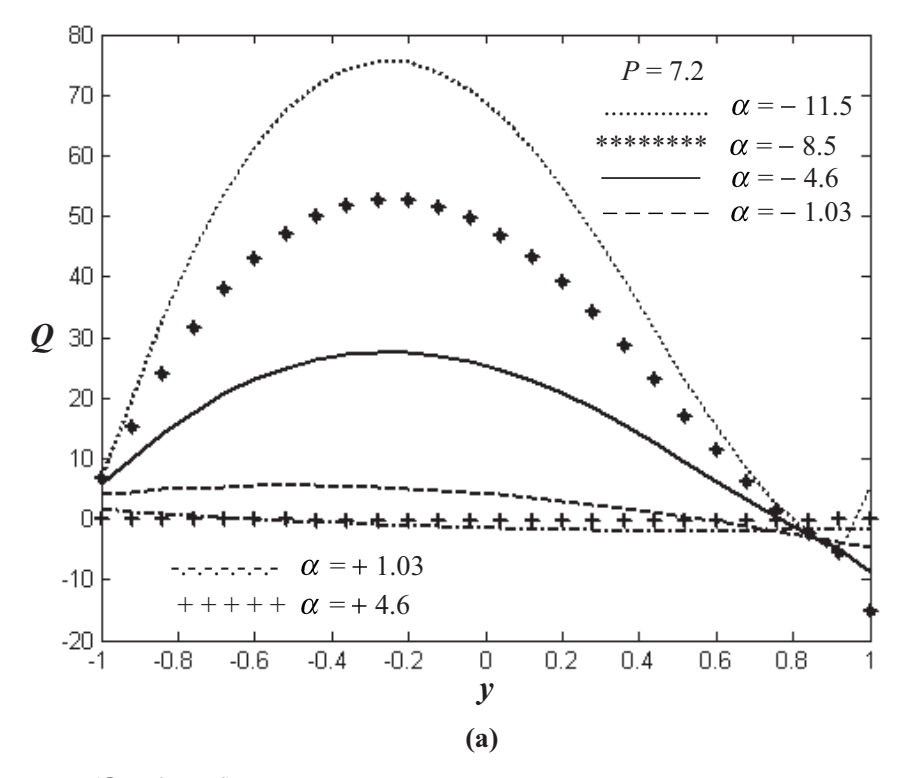


Figure 11: (Continued)

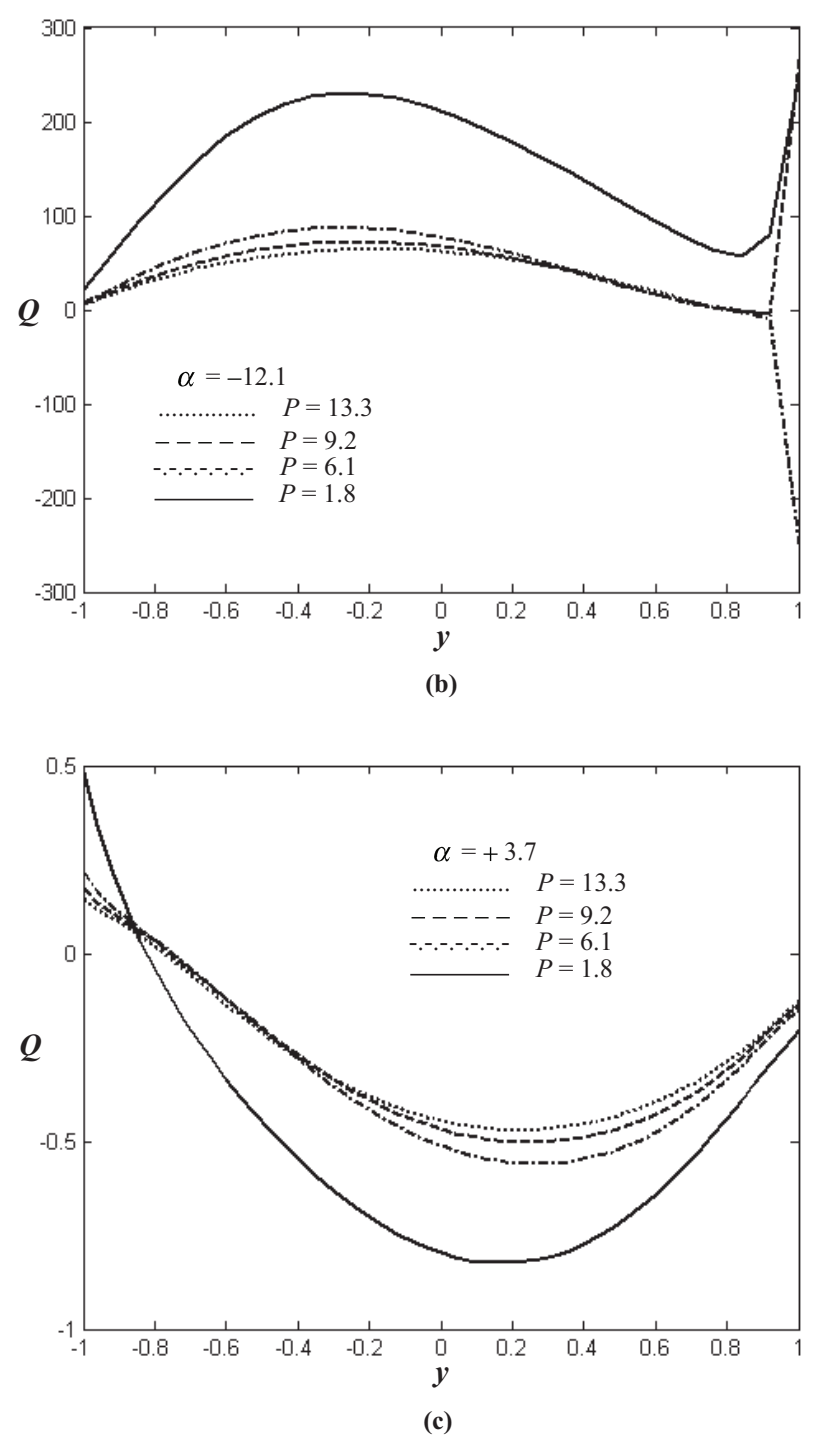


Figure 11: Normal pressure gradients distribution: (a) for P = 7.2 under various values of the sensitivity of viscosity to thermal variations, (b) for α = -12.1 under different values of the Péclet number, (c) for α = +3.7 under different conductivities

negative sensitivities of viscosity to thermal variations, since very rapid variations occur near the hot wall.

The behavior of the normal pressure gradient for different conductivities at a fixed negative parameter α as plotted in Fig. 11(b) is reversed in Fig. 11(c) with a positive fixed parameter α . More precisely, in Fig. 11(c), normal pressure gradients decrease at the vicinity of the cold wall and increase near the hot wall. Furthermore, Fig. 11(c) shows that the increase of function Q with the Péclet number is very noticeable away from the cold wall. This characteristic of the normal pressure gradients presented in Fig. 11(c) is contrary to that of Fig. 11(b) in a large area away from both walls.

6. CONCLUSION

The flow process or the fluid motion manifests itself at the macroscopic level as a phenomenon of mass distribution combined with thermal conduction and convection. The diffusion of momentum occurs due to the rubs of fluid layers from each other and the diffusion coefficient associated is the dynamic viscosity or the shear viscosity. This shear viscosity is at the origin of friction effects when the fluid is in contact with a solid wall. The investigation of flows between two parallel porous walls kept at different temperatures is interesting as the fluid is driven by suction while the dynamic viscosity varies with temperature. The theory is indispensable to ensure a deeper understanding of such problems as done in this work. It is found that, since wall suction and flow reversal occur concurrently, some collision zones exist in the channel. In fact, the simultaneous existence of wall suction and the backward flow is an attempt of mass conservation to be satisfied within the channel. Indeed, the scenario of mass conservation is the one for which a given fluid particle which leaves the channel by suction motion is replaced with another particle in order to occupy the empty space thus created due to the reverse flow. Since the streamwise velocity is in many cases negative according to the numerical results obtained, this leads to conclusion that the effect of flow reversal is dominant on that of suction. This domination holds only when the fluid flows with high viscosity. The difference of temperatures causes different behaviors in terms of flow characteristics at the vicinity of both walls of the channel by referring to the evolution of the transverse pressure gradient which is very sensitive to high temperature near the hot wall for certain values of control parameters. The normal pressure gradients diminish with the increase of the sensitivity of viscosity to thermal variations at a given conductivity, reason why the backward flow is very important for positive values of the parameter α .

REFERENCES

- [1] Taylor, C. L., Banks, W. H. H., Zaturska, M. B. and Drazin, P. G., Three-dimensional Flow in a Porous Channel, *Quarterly Journal of Mechanics and Applied Mathematics*, 1991, 44(1), 105–133.
- [2] Zaturska, M. B. and Banks, W. H. H., Suction-driven Flow in a Finite Wedge, *Acta Mechanica*, 1991, 86, 95–101.
- [3] Berman, A. S., Laminar Flow in Channels with Porous Walls, *Journal of Applied Physics*, 1953, 24(9), 1232–1235.
- [4] Sellars, J. R., Laminar Flow in Channels with Porous Walls at High Suction Reynolds Number, *Journal of Applied Physics*, 1955, 26(4), 489–490.
- [5] Proudman, I. and Johnson, K., Boundary-layer Growth at a Rear Stagnation Point, *Journal of Fluid Mechanics*, 1962, 12(2), 161–168.

- [6] Terrill, R. M., Laminar Flow in Uniformly Porous Channel, *Aeronautical Quarterly*, 1964, 15(3), 299–310.
- [7] Terrill, R. M. and Shrestha, G. M., Laminar Flow through Parallel and Uniformly Porous Walls of Different Permeability, *Journal of Applied Mathematics and Physics*, 1965, 16(4), 470–482.
- [8] Durlofsky, L. and Brady, J. F., The Spatial Stability of a Class of Similarity Solutions, *Physics of Fluids*, 1984, 27(5), 1068–1076.
- [9] MacGillivray, A. D. and Lu, C., Asymptotic Solution of a Laminar Flow in a Porous Channel with Large Suction: A Nonlinear Turning Point Problem, *Methods and Applications of Analysis*, 1994, 1(2), 229–248.
- [10] Zhou, C. and Majdalani, J., Improved Mean-flow Solution for Slab Rocket Motors with Regressing Walls, *Journal of Propulsion and Power*, 2002, 18(3), 703–711.
- [11] Robinson, W. A., The Existence of Multiple Solutions for the Laminar Flow in a Uniformly Porous Channel with Suction at Both Walls, *Journal of Engineering Mathematics*, 1976, 10(1), 23–40.
- [12] Ferro, S. and Gnavi, G., Spatial Stability of Similarity Solutions for Viscous Flows in Channels with Porous Walls, *Physics of Fluids*, 2000, 12(4), 797–802.
- [13] Li, B., Zheng, L., Zhang, X. and Ma, L., The Multiple Solutions of Laminar Flow in a Uniformly Porous Channel with Suction/Injection, *Advanced Studies in Theoretical Physics*, 2008, 2(10), 473–478.
- [14] Majdalani, J. and Zhou, C., Moderate-to-large Injection and Suction Driven Channel Flows with Expanding and Contracting Walls, *ZAMM*, 2003, 83(3), 181–196.
- [15] Zaturska, M. B., Drazin, P. G. and Banks, W. H. H., On the Flow of a Viscous Fluid Driven along a Channel by Suction at Porous Walls, *Fluid Dynamics Research*, 1988, 4(3), 151–178.
- [16] Gol'dshtik, M. A. and Ersh, N. M., Stability of Pipe Flow with Blowing, *Fluid Dynamics*, 1989, 24(1), 51–59.
- [17] Terrill, R. M. and Thomas, P. W., On Laminar Flow through a Uniformly Porous Pipe, *Applied Scientific Research*, 1969, 21(1), 37–67.
- [18] Brady, J. F., Flow Development in a Porous Channel or Tube, *Physics of Fluids*, 1984, 27(5), 1061–1067.
- [19] Banks, W. H. H. and Zaturska, M. B., On Flow through a Porous Annular Pipe, *Physics of Fluids A*, 1992, 4(6), 1131–1141.
- [20] Majdalani, J. and Flandro, G. A., The Oscillatory Pipe Flow with Arbitrary Wall Injection, *Proceedings of the Royal Society of London A*, 2002, 458, 1621–1651.
- [21] Hona, J., Ngo Nyobe, E. and Pemha, E., Dynamic Behavior of a Steady Flow in an Annular Tube with Porous Walls at Different Temperatures, *International Journal of Bifurcation and Chaos in Applied Sciences and Engineering*, 2009, 19(9), 2939–2951.
- [22] Hona, J., Pemha, E. and Ngo Nyobe, E., Viscous Flow and Heat Transfer through Two Coaxial Porous Cylinders, *International Journal of Multiphysics*, 2015, 9(1), 45–60.
- [23] Ockendon, H. and Ockendon, J. R., Variable-viscosity Flows in Heated and Cooled Channels, *Journal of Fluid Mechanics*, 1977, 83, 177–190.

- [24] Schäfer, P. and Herwig, H., Stability of Plane Poiseuille Flow with Temperature Dependent Viscosity, *International Journal of Heat and Mass Transfer*, 1993, 36(9), 2441–2448.
- [25] Lin, C.-R. and Chen, C.-K., Effect of Temperature Dependent Viscosity on the Flow and Heat Transfer over an Accelerating Surface, *Journal of Physics D*, 1994, 27(1), 29–36.
- [26] Wylie, J. J. and Lister, J. R., The Effects of Temperature Dependent Viscosity on Flow in a Cooled Channel with Application to Basaltic Fissure Eruptions, *Journal of Fluid Mechanics*, 1995, 305, 239–261.
- [27] Pemha, E., Hona, J. and Ngo Nyobe, E., Numerical Control of a Two-dimensional Channel Flow with Porous Expanding Walls at Different Temperatures, *International Journal of Flow Control*, 2014, 6(4), 119–134.
- [28] Brown, H. R., Rayleigh-Taylor Instability in a Finite Thickness Layer of a Viscous Fluid, *Physics of Fluids A*, 1989, 1(5), 895–896.
- [29] Davis, A. M. J. and Frenkel, A. L., Cylindrical Liquid Bridges Squeezed between Parallel Plates: Exact Stokes Flow Solutions and Hydrodynamic Forces, *Physics of Fluids A*, 1992, 4(6), 1105–1109.
- [30] Brady, J. F. and Acrivos, A., Steady Flow in a Channel or Tube with an Accelerating Surface Velocity. An Exact Solution to the Navier-Stokes Equations with Reverse Flow, *Journal of Fluid Mechanics*, 1981, 112, 127–150.
- [31] Stewartson, K., *The Theory of Boundary Layers in Compressible Fluids*, Oxford University Press, Oxford, 1964.